INVITED PAPER

THz-Wave Spectroscopy Applied to the Detection of Illicit Drugs in Mail

Chemical powders in envelopes can be identified by THz-wave spectrum analysis, a process that can be speeded-up by rapid scanning to determine whether powders are present.

By Adrian Dobroiu, Yoshiaki Sasaki, Takayuki Shibuya, Chiko Otani, and Kodo Kawase, *Member IEEE*

ABSTRACT | A series of experiments in the field of THz-wave spectroscopy is described. The measurement of absorption spectra of solid samples, powders, and liquids is demonstrated using various optical setups. One of the sources we used is a widely tunable coherent THz-wave generator relying on an optical parametric process: nanosecond Q-switched Nd : YAG laser light scattering from the polariton mode of a MgO-doped $LiNbO_3$ crystal. For the measurement of the absorption of THz waves in liquids, a train of waves is allowed to oscillate inside a silicon prism. A liquid placed on a total internal reflection surface lowers the quality factor of the resonator, which allows determining the complex refraction index of the sample by frequency scanning. We have also developed a technique for THz chemical imaging, by introducing the component spatial pattern analysis. The spatial distribution of the chemicals, such as illicit drugs concealed in an envelope, is obtained from terahertz multispectral transillumination images and absorption spectra. To compensate for the low imaging speed, a prescreening step is proposed, by first detecting the presence of powders in the envelopes, which is achieved by measuring in real time the amount of scattering produced by the envelopes. Details and examples are provided.

KEYWORDS | Homeland security; nondestructive testing; terahertz spectroscopy; terahertz waves; terahertz-wave sources

Manuscript received October 28, 2005; revised March 22, 2007. This work was supported in part by the Asian Office of Aerospace Research and Development under Grant AOARD-05-4023.

A. Dobroiu, **Y. Sasaki**, **T. Shibuya**, and **C. Otani** are with the Institute of Physical and Chemical Research (RIKEN), Sendai 980-0845, Japan (e-mail: dobroiu@riken.jp; ysasaki@riken.jp; shibuya@riken.jp; otani@riken.jp).

K. Kawase is with the Graduate School of Engineering, Nagoya University, Nagoya 464-8603, Japan (e-mail: kodo@riken.jp).

Digital Object Identifier: 10.1109/JPROC.2007.898840

I. INTRODUCTION

Until very recently, terahertz (THz) radiation was the exotic and largely unknown field at the gap between high frequency millimeter waves and long wavelength infrared, that only few investigators had the opportunity to explore. As new sources and detectors have emerged, increasingly numerous research teams have started to find applications that respond to the real-world challenges of our times.

Among the most prominent advantages that the THz radiation offers we mention its ability to penetrate a wide range of materials—plastics, wood and paper, fabric, semiconductors, and many others—which are opaque to visible and near infrared light or produce only low-contrast x-ray images. As the THz photon energy is roughly six orders of magnitude smaller than that of an x-ray photon, its interaction with matter, particularly with biological tissues, is considered to cause no detectable damage, at least not by ionization processes. A comparison with the other side of the electromagnetic spectrum, the microwave range, highlights again the advantage of THz waves: with their shorter wavelength they provide a considerably better imaging resolution that is sufficient in many applications [1]. The existence of chemically specific absorption spectra in the THz range, reflecting molecular transitions and intermolecular bonds, facilitates fingerprinting and brings about a whole area of spectroscopic detection, testing, and analysis techniques. THz spectroscopy can qualitatively and quantitatively characterize the chemical composition of a sample [2] with applications such as the noninvasive detection of illegal drugs hidden in envelopes [3]. The absorption of THz waves by water, although usually a limiting factor, can be exploited in other applications such as monitoring of water contents

in plants for the agriculture. High expectations regarding THz imaging come also from medicine [4].

II. THz-WAVE SOURCES

Generation of THz waves in the laboratory is obtained, more often than not, by optical rectification or photoconductive switching produced using femtosecond laser pulses. Applied research, such as time-domain spectroscopy, makes use of the high time resolution of THz-waves and ultrabroad bandwidth up to the THz region. While this technique has qualities such as room temperature operation, wide spectrum, and easy access to the wave phase, it still suffers from bulkiness and low speed. Several areas or research require monochromatic sources that are also easy to use and compact.

A. Parametric Generators

A technique for producing THz radiation, which has brought about several kinds of sources, is the so-called parametric generation. The THz wave is emitted based on an optical parametric process in a nonlinear crystal [5], [6]. The THz-wave parametric generator (TPG) [7], THz-wave parametric oscillator (TPO), and injection seeded TPG (is-TPG) making use of this principle are not only compact but also operate at room temperature, and are suitable as practical radiation sources. Moreover, the nanosecond THz-wave pulse, determined by the Q-switched laser pulse used for pumping, offers the potential advantage of a narrow linewidth over the femtosecond THz-wave pulses of other sources. In principle, both a narrow linewidth and a wide tunability are possible in injection-seeded TPG systems with single-longitudinal mode near-infrared lasers as pump sources and seeders. Details about TPG, TPO, and is-TPG are given in [8].

When an intense laser beam propagates through a nonlinear crystal, photon and phonon transverse wave fields are coupled, and behave as new mixed photon-phonon states, called polaritons. The generation of the THz radiation results from the efficient parametric scattering of laser light via a polariton, that is, stimulated polariton scattering. The scattering process involves both second- and third-order nonlinear processes. Thus, strong interaction occurs among the pump beam, the idler beam, and the polariton (THz) waves.

One of the most suitable nonlinear crystals to generate THz-wave is $LiNbO_3$ thanks to its large nonlinear coefficient [9] ($d_{33} = 25.2$ pmV^{-1} at $\lambda = 1.064$ μm) and its transparency over a wide wavelength range (0.4 to 5.5 μm). $LiNbO_3$ has four infrared- and Raman-active transverse optical (TO) phonon modes, called A_1-symmetry modes, and the lowest mode ($\omega_0 \sim 248$ cm^{-1}) is useful for efficient far-infrared generation because it has at the same time the largest parametric gain and the smallest absorption coefficient.

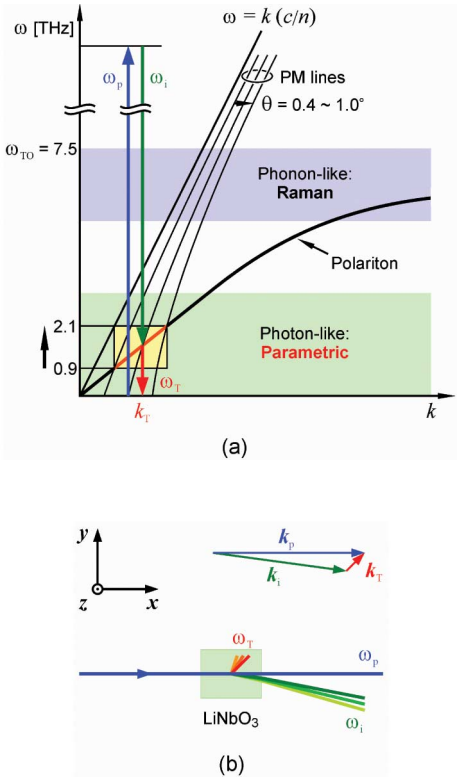

Fig. 1. ***Dispersion relation of the polariton. (a) An elementary excitation is generated by the combination of a photon and a transverse optical phonon*** (ω_{TO})***. The polariton in the low energy region behaves like a photon at THz frequency. Due to the phase-matching condition as well as the energy conservation law which hold in the stimulated parametric process, tunable THz waves are obtained by controlling of the wave vector*** k_i***. (b) The noncolinear phase-matching condition. (After [8].)***

The principle of tunable THz-wave generation is as follows. Polaritons exhibit phonon-like behavior in the resonant frequency region (near the TO-phonon frequency ω_{TO}). However, they behave like photons in the non resonant low-frequency region, as shown in Fig. 1(a), where a signal photon at THz frequency and a near-infrared idler photon are created parametrically from a near-infrared pump photon, according to the energy conservation law

$$\omega_p = \omega_T + \omega_i, \tag{1}$$

where subscripts mean pump, THz, and idler, in this order. In the stimulated scattering process, the momentum conservation law, expressed as a noncollinear phase-matching condition

$$\mathbf{k}_p = \mathbf{k}_T + \mathbf{k}_i, \tag{2}$$

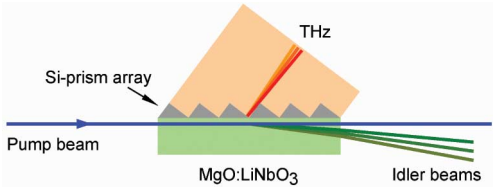

Fig. 2. *A THz-wave parametric generator (TPG) with a silicon prism array placed on the lateral surface of the $LiNbO_3$ to increase the output and to reduce the diffraction angle of the THz wave by maximizing the coupling area. Since this setup does not use any frequency selection device, the generated THz radiation generated contains a wide range of frequencies. (After [1].)*

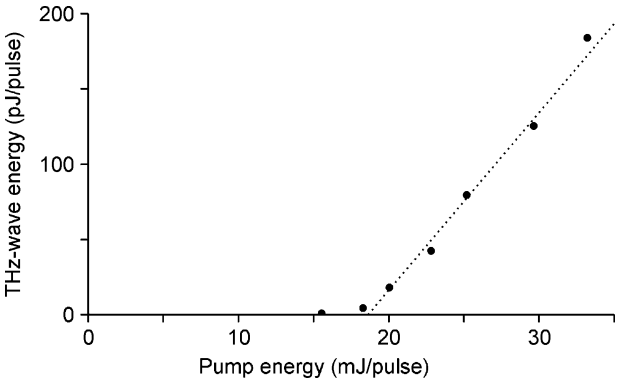

Fig. 4. *Input–output characteristics of a TPO. (After [8].)*

also holds. This leads to the angle-dispersive characteristics of the idler and THz waves [see Fig. 1(b)]. A primitive THz-wave generator is shown in Fig. 2; it uses just the nonlinear crystal placed in the pump beam. The output of such a device contains a wide range of frequencies as there is no frequency selector in place. For an efficient extraction of the THz wave from inside the crystal several techniques have been tried, and the one presented in the figure, making use of an array of small silicon prisms, seems to be most suitable. The prism array covers the whole lateral surface of the crystal, increasing the collection efficiency, and minimizing the diffraction effects.

A coherent THz wave is generated efficiently by selecting a narrow fragment of the wide range THz spectrum that is emitted. This is achieved either by using an optical resonator, or by seeding the idler wave in a process called injection seeding. Continuous and wide tunability is accomplished simply by changing the angle between the incident pump beam and the resonator axis and in the second case also the seed wavelength.

B. The Terahertz-Wave Parametric Oscillator

Coherent tunable THz waves can be generated by realizing a resonant cavity for the idler wave. This is the basic configuration of a TPO, and it consists of a Q-switched Nd : YAG laser, the nonlinear crystal, and a parametric oscillator, as shown in Fig. 3. The idler wave is amplified in the resonator consisting of flat mirrors with a half-area HR coating. The mirrors and crystal are installed on a precise, computer-controlled rotating stage for precise tuning. When the incident angle of the pump beam into the $LiNbO_3$ is varied between 3.13 and 0.84 deg, the angle between the pump wave and the idler wave in the crystal changes from 1.45 down to 0.39 deg, whereas the angle between the THz-wave and the idler wave changes from 67.3 down to 64.4 deg. With this slight variation in the phase-matching condition, the wavelength (frequency) of the THz-wave could be tuned between 100 and 330 μm (0.9 to 3.0 THz); the corresponding idler wavelength changed from 1.075 down to 1.067 μm.

Typical input–output characteristics of a TPO are shown in Fig. 4, where it can be seen that the oscillation threshold was 18 mJ/pulse. With a pump power of 34 mJ/pulse, the output energy of THz wave from TPO was 192 pJ/pulse ($\cong$ 19 mW at the peak), calibrated using the sensitivity of the bolometer. Since the Si-bolometer output becomes saturated at approximately 5 pJ/pulse, we used several sheets of thick paper as an attenuator after they were properly calibrated. The minimum sensitivity of the Si-bolometer is approximately 1 fJ/pulse; therefore, the dynamic range of measurement using the TPO as a source is from 1 fJ to 192 pJ (about 53 dB).

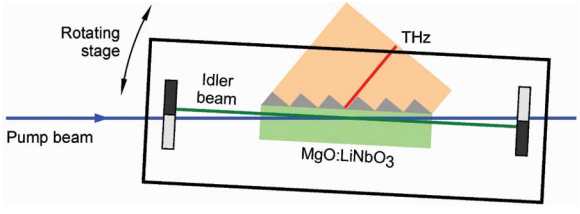

Fig. 3. *TPO configuration. The TPO consists of a Q-switched Nd : YAG laser, a nonlinear crystal, and a resonator. The idler wave is amplified in the resonator consisting of two flat mirrors, both with a half-area HR coating. The mirrors and crystal are installed on a precise computer-controlled rotating stage for fine tuning. (After [8].)*

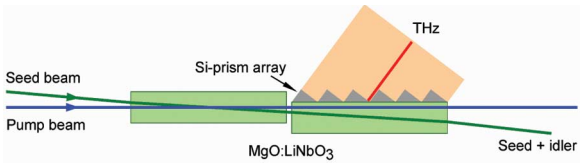

Fig. 5. *Experimental setup of the is-TPG. (After [8].)*

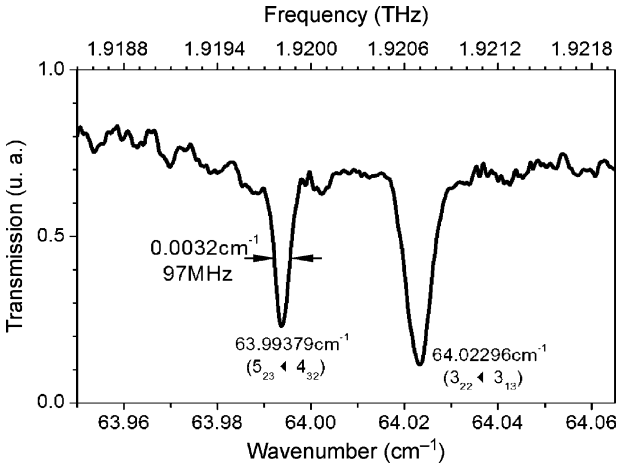

Fig. 6. *An example of the absorption spectrum measurement of low-pressure (< 1 torr) water vapor at around 1.92 THz. Resolution of less than 100 MHz (0.003 cm $^{-1}$) was clearly demonstrated. The transmission values are given in arbitrary units; the absorption peaks should have given an almost zero transmission, however this was prevented by the limited resolution and frequency stability. (After [8].)*

C. The Injection-Seeding Terahertz-Wave Parametric Generator

In the is-TPG, the THz spectrum specific to a TPG source is narrowed to the Fourier transform limit imposed by the pulse length by introducing the injection seeding for the idler wave. Fig. 5 shows our experimental setup of the is-TPG. The purity of the THz-wave frequency is dramatically improved. Simultaneously, the output power obtained is several hundred times higher than that of a conventional TPG. In addition, wide tunability and fine resolution were demonstrated using a tunable seeder. The THz-wave output energy and the temporal waveform were measured with a 4K Si bolometer and a Schottky barrier diode detector, respectively.

It was possible to tune the THz wavelength using an external cavity laser diode as a tunable seeder. A wide tunability, from 125 to 430 μm (0.7 to 2.4 THz), was achieved by changing simultaneously the seed wavelength and the seed incident angle.

The absorption spectrum of low-pressure (<1 torr) water vapor was measured to demonstrate the continuous tunability and the high resolution of the is-TPG. The absorption gas cell used was an 87-cm-long stainless steel pipe with TPX windows at both ends. Fig. 6 shows an example of measurements around 1.92 THz, where two neighboring lines exist. Resolution of less than 100 MHz (0.003 cm^{-1}) was clearly shown. Such a resolution can be achieved with FTIR spectrometers having a long scanning distance; however, especially for narrow frequency ranges, the time required by an is-TPG-based spectrometer is considerably shorter.

The system is capable of continuous tuning at high spectral resolution in 4 GHz segments anywhere in the region from 0.7 to 2.4 THz. Since there is no cavity the continuous tuning is extendible, in principle, to the full tunability of the is-TPG by using a mode-hop-free seeder, such as a Littman-type external cavity diode laser.

The input–output characteristic of the THz wave from an is-TPG is shown in Fig. 7. The maximum conversion efficiency was achieved when the pump and seed beams almost fully overlapped at the incident surface of the first MgO:$LiNbO_3$ crystal. The maximum THz-wave output of 1.3 nJ/pulse (peak power over 300 mW) was obtained with a single-mode pump beam of 34 mJ/pulse and a seed beam of 50 mW. To prevent saturating the Si bolometer, again we used several sheets of thick paper as an attenuator after calibrating them. In our previous studies, the maximum THz-wave output from a conventional TPG and a TPO was 1 and 190 pJ/pulse, respectively [10]. The Si bolometer became saturated at about 5 pJ/pulse, so we used several thick calibrated sheets of paper as an attenuator. As the minimum sensitivity of the Si-bolometer is about 1 fJ/pulse, the dynamic range of the is-TPG system was from 1.2 nJ down to 1 fJ, that is, around 60 dB, which is sufficient for most applications. The dynamic range can be significantly increased using a lock-in amplifier.

D. Other Sources

Apart from a THz time-domain spectroscopy system, both in our imaging [11] and spectroscopic [12] experiments we have also used a backward-wave oscillator (BWO), which has the advantages of high output power, continuous wave, clean wavefront, and ease of operation. In a few words, the BWO operates as follows. A heated cathode emits electrons that are focused by a strong magnetic field and drawn toward the anode through a comb-like decelerating structure. As a result, an electromagnetic wave is produced that travels in the opposite

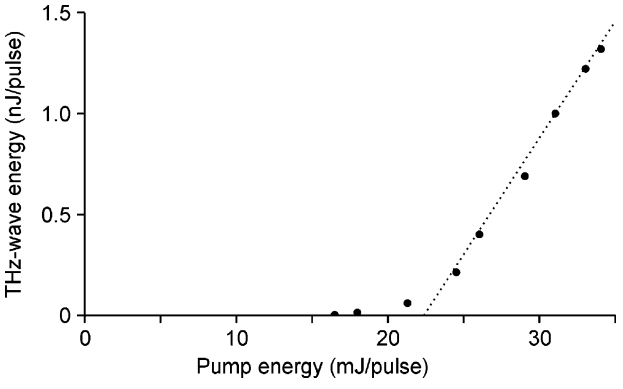

Fig. 7. *Input–output characteristics of the is-TPG. Compared to the TPO characteristic graph in Fig. 4, the output of the is-TPG is almost an order of magnitude stronger. (After [1].)*

direction (hence the name) and couples into a curved waveguide that takes it out into free space. The output frequency depends on the electron speed, which is determined by the voltage applied between the electrodes, allowing about 30% tunability around the central frequency.

Another source that we used in our experiments is a microwave oscillator followed by a chain of frequency multipliers and amplifiers (Virginia Diodes, Inc.). Its frequency can be tuned in the range from 600 to 665 GHz, and the RF output power is about 70 μW.

III. SPECTROSCOPY

Several techniques of characterizing a material from the viewpoint of its absorption in the THz range are discussed below. The choice of one method or another is determined by the material, as bulk solids, powders, liquids, and gasses require specific investigation methods; it is equally important whether the material is weakly or highly absorptive.

A. Transmission Spectroscopy

For solid samples, whether they are in the form of bulk material, such as plates, sheets, and pellets, or in powder, one of the simplest ways to measure the absorption spectra is by using transmission spectroscopy. The THz beam incident on the sample is partly transmitted, and the ratio of attenuation, combined with information about the thickness and concentration of the sample, allows the determination of the absorption coefficient of the material under study. For the particular case considered in this report, illicit drugs and explosives among others have been analyzed, with the purpose of creating a database of THz fingerprint spectra of various chemicals of interest. Fig. 8 shows a few absorption spectra, which are a clear demonstration that THz spectroscopy can help identify an unknown chemical by recording its absorption spectrum.

One disadvantage of this technique consists in the fact that, in plate or pellet samples, repeated internal reflections inside the sample can, in certain conditions, generate an etalon effect, seen in the transmission spectra as frequency-periodic oscillations. The effect is stronger for homogeneous samples with flat and parallel surfaces, especially if they are made of a material with low absorption and large refraction index, because such samples allow a wave to resonate a significant number of times.

B. Diffuse Reflection

Sometimes it is difficult to apply the transmission method for powder samples, since the scattering effect can be strong enough to reduce the amount of transmitted power even for relatively thin samples. In such cases the diffuse reflection method can give better results, particularly for thick samples.

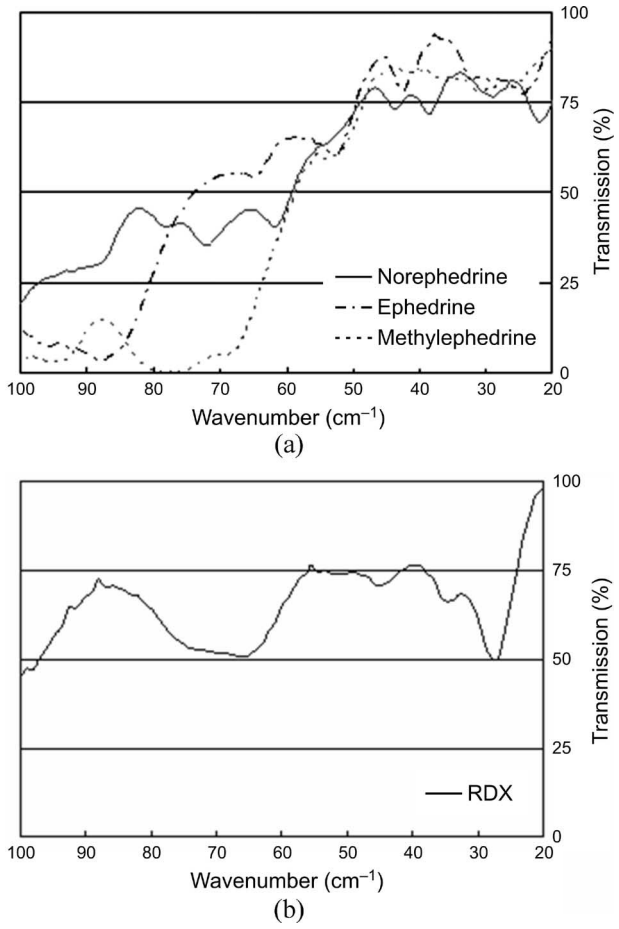

Fig. 8. *Fingerprint spectra of: (a) methamphetamine-based illicit drugs and (b) that of an RDX explosive, all measured with an FTIR spectrometer. The samples are polyethylene-based pellets, with a thickness between 1 and 2 mm. The spectral features seen in these graphs do not depend significantly on the sample thickness and concentration, and thus could be used for chemical identification.*

The diffuse reflection technique consists in measuring the reflection from a rough surface, onto which a collimated incident beam is scattered in all directions. The diffuse reflection can be used to measure the absorbance, and we tested whether a fingerprint spectrum could be obtained from the diffuse reflection spectrum of a powder. We used an ordinary FTIR spectrometer to which a diffuse reflection unit was attached. Fig. 9 shows the result of such measurement. The absorbance peaks appears at the same wave numbers as in the transmission measurements, which confirms the applicability of the diffuse reflection to our inspection purpose.

C. Spectroscopy of Liquids

Whether for chemical analysis in the laboratory, for homeland security, or other purposes, liquid spectroscopy can prove important in many areas of research and industry. The physical properties of water for example

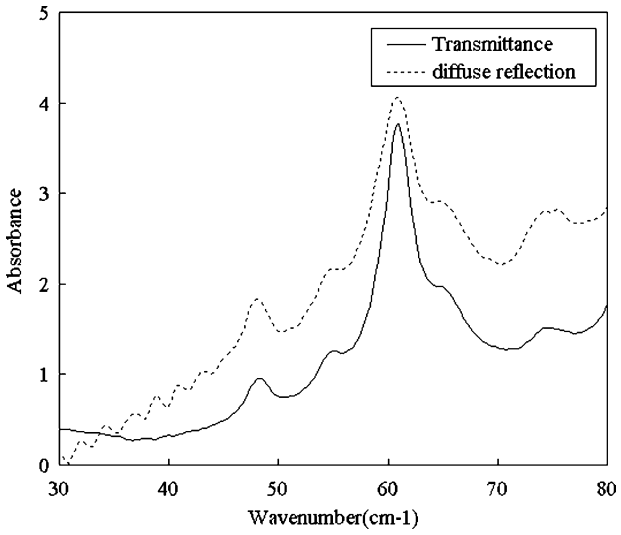

Fig. 9. *Sucrose absorption spectra, measured in diffuse reflection (dotted line) and transmission (solid line). Both spectra were recorded using an FTIR system; the absorbance values are given in arbitrary units different for each sample, to allow comparison.*

have drawn the attention of investigators for a long time, and THz measurements have a definite potential in understanding its properties. We describe here two methods for obtaining transmission data in liquids, one based on a special type of cell, and the other on a particular type of interferometer.

Wedge-Shaped Cell: The measurement of the transmission spectra of liquids requires special cells in which those liquids are inserted. Various techniques are available, such as using a cell of adjustable thickness [13]. As cells with uniform thickness usually suffer from the etalon effect, one widespread solution is to use wedge-shaped cells [14] and focus the radiation on a small area of the cell. Using this technique and a BWO-based THz imaging system we measured for example the absorption coefficient of water around 600 GHz. A layer of water whose thickness varies from 0 to 564 μm was produced by joining two 0.15 mm thick glass slides so that they touch each other on one edge and are spaced at the other, and filling with water the volume between; the water is retained by surface tension. The beam is focused normally on the wedge surface and the transmitted signal is recorded as the wedge is scanned from the thin end to the thick end. Because the glass thickness is constant, the only variable absorption effect comes from water. If the etalon effect inside the water is neglected the transmitted intensity will have a simple exponential dependence on the position

$$I(x) = I_0 e^{-\alpha\theta x} \tag{3}$$

where x is the position of the focused beam, starting from where the water thickness is zero, I_0 is the transmitted intensity at $x = 0$, α is the absorption coefficient, and θ is the wedge angle in radians.

Fig. 10 shows an example of a typical scan [11]. We obtained for the absorption coefficient of water (temperature 23 °C, frequency 593.5 GHz) the value of 181 ± 9 cm^{-1}, which agrees to the value given by the literature [15]: 174.8 cm^{-1}.

Monolithic Fabry–Pérot Resonator: Another measurement technique for the absorption of THz waves in liquids is by using a silicon prism in which a train of waves is allowed to reflect back and forth as in a Fabry–Pérot resonator [12] (Fig. 11). The sensing element, a high-resistivity silicon prism having the angles of 45°, 45°, and 90°, is placed in the collimated beam of a BWO source. On the upper surface the wave undergoes a total internal reflection, while the lateral surfaces only give a partial Fresnel reflection of about 30%, which is nevertheless sufficient for sustaining several oscillations of the wave inside the prism.

When a liquid is placed on the total internal reflection surface of the prism, the quality factor of the resonator decreases, and the measurement of this decrease allows determining the complex refraction index of the sample. The measurement is done by scanning the BWO frequency within a short interval and Fourier processing of the data, as shown in Fig. 12. We relied on the property of the Airy function that when its Fourier transform is calculated, the ratio between the consecutive peaks is

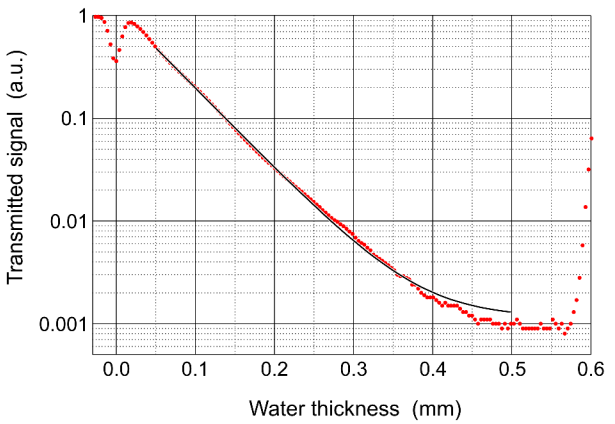

Fig. 10. *Scan of a wedge-shaped cell with water. The dots correspond to the measurement data and the continuous curve shows the fit using a formula similar to (3) with an additive parameter to account for electronic offset. This curve gives the value of the absorption coefficient of water. The small dip at zero thickness is the shadow of the edge of the upper glass sheet. The fitting error seems unbalanced due to the logarithmic vertical scale. (After [11].)*

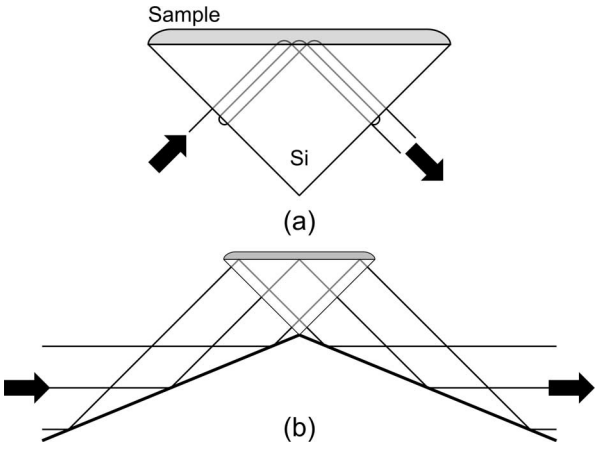

Fig. 11. *(a) Silicon prism placed in (b) a collimated beam. The repeated internal reflections make the prism act as a Fabry–Pérot resonator. A liquid sample placed on the surface of total internal reflection modifies the quality factor of the resonator. (After [12].)*

equal to the square root of the energy loss ratio in a full loop.

The remarkable feature of this interferometer is that although it is realized as a solid piece of material containing the wave in its volume, it still allows the sample to be placed *inside* the cavity. Additionally, the layer of sample can have any thickness provided that it is above a certain minimum limit which depends on the absorption properties of the liquid. The etalon effect that is a nuisance in other measurement configurations does not manifest itself in our setup.

To demonstrate the efficiency of this technique we performed for example a series of measurements on water-ethanol solutions of various concentrations, and plotted the power loss at the total internal reflection surface versus the ethanol concentration. The graph, given in Fig. 13, shows that the method could be used for example in measuring the concentration of an unknown solution, by reversing the relationship. Up to about 70% ethanol concentration the measurement of an unknown solution gives an error between 3% and 5% in the present conditions. Additional tests have shown that the method can be used for other solutions as well.

IV. CHEMICAL IMAGING

We have previously reported [2] on the development of a novel basic technology for THz imaging, which allows the detection and identification of chemicals by introducing the component spatial pattern analysis. The spatial distribution of the chemicals is obtained from terahertz multispectral transillumination images, also using absorption spectra previously measured with our widely tunable THz-wave parametric oscillator.

We have applied this technique, for example, to the detection and identification of illicit drugs concealed in envelopes. Fig. 14 shows the optical setup used for such a measurement, relying on a TPO as source, a pyroelectric detector, and mechanical scanning of the sample. Transmission images recorded at several frequencies, shown as absorption data in Fig. 15, are processed using the component spatial pattern analysis. The result, shown in Fig. 16, demonstrates that the spatial distribution of each chemical can be recovered precisely. As this measurement was done with the sample inside a usual paper envelope, the practical application to the *noninvasive* detection of illicit drugs in mail dispatching centers only requires the implementation of the technology in practice.

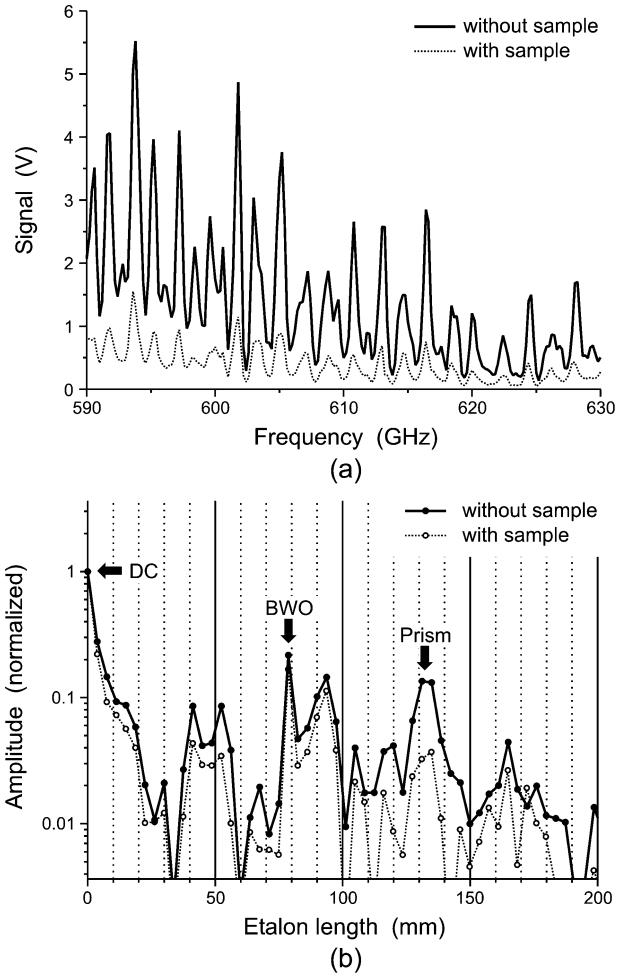

Fig. 12. *The effect of a liquid on the evanescent wave. The spectrum (a) changes not only because the liquid absorbs part of the radiation, but also because of a decreased quality factor of the resonator. The Fourier transform (b) reveals the peak corresponding to the etalon effect inside the prism. The peak marked BWO is attributed to Fabry–Pérot oscillations inside the source. (After [12].)*

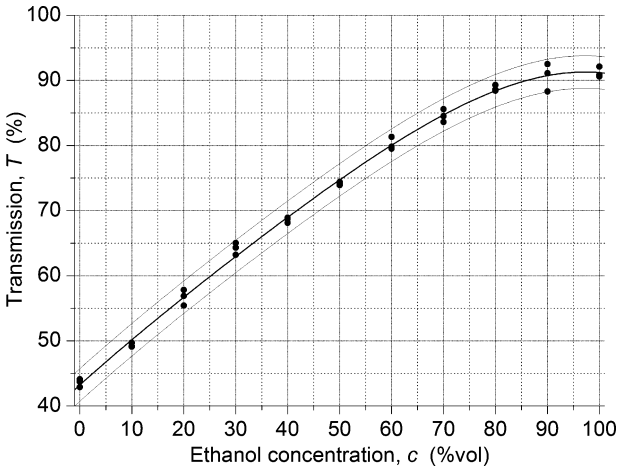

Fig. 13. *The power loss at the total internal reflection surface, denoted by T, as a function of the ethanol concentration. Three measurements were made for each concentration. The leftmost data points correspond to pure water, and the rightmost points to pure ethanol. Toward the high ethanol concentration end the slope of the curve becomes small, so that measuring the concentration of an unknown solution cannot be done accurately, but under 70% the error is less than 5%. (After [12].)*

V. SCATTERING

Since the low speed of mail imaging would be a bottleneck in a real-life mail screening process, we proposed a prescreening step. This is achieved by first detecting the presence of powders in the envelopes, because it is known that many of the illicit drugs sent through mail are in powder form. The presence of powders is determined by measuring the amount of THz-wave scattering produced by each envelope on the conveyer belt. Our experiments show that real-time screening is possible.

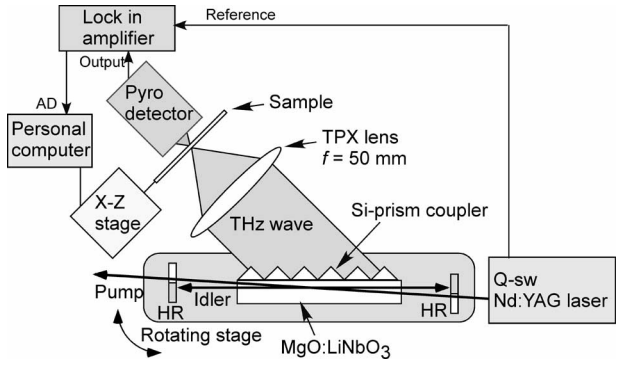

Fig. 14. *The optical setup used in chemical imaging. A TPO was used as source and a pyroelectric sensor detected the transmission images. A computer controls the xy stage movement and signal acquisition and processing. (After [3].)*

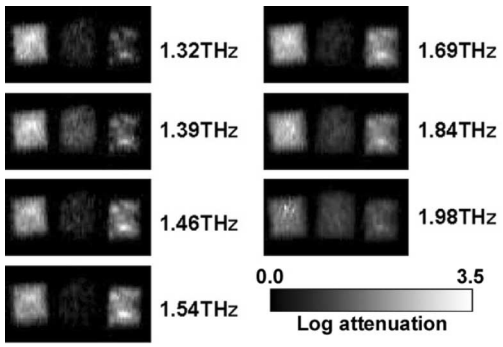

Fig. 15. *The multispectral absorption image of a sample consisting of three small plastic bags. The bags contain, from left to right: MDMA, aspirin, and methamphetamine. (After [3].)*

A simple test setup is shown in Fig. 17, where a TPO is used a source and the detection is realized with a silicon bolometer. The beam transmitted through the sample, with no scattering, is removed by focusing it into a damper. Part of the scattered radiation is collected and measured. Such a system, optimized to remove most of the direct beam, and to collect the scattered waves as much as possible, is prepared to be implemented in a post office distribution center; its prototype uses a frequency multiplied source and a Schottky diode detector. The envelopes will pass through the THz beam and as soon as a significant amount of scattered waves are detected, the envelope in question is automatically taken away from the main conveyor belt and further analyzed (using a combination of methods that

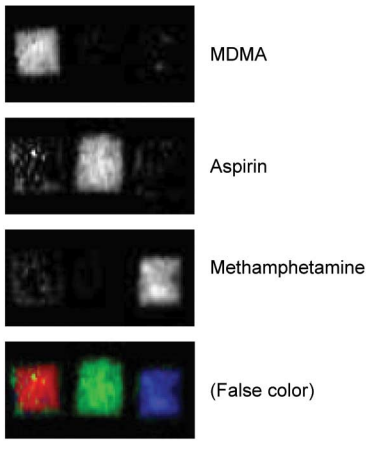

Fig. 16. *Result after processing the multispectral transmission image. Brighter shades of gray mean higher concentration of the respective chemical. The spatial distribution calculated separately for each drug accurately matches that of the sample. (After [3].)*

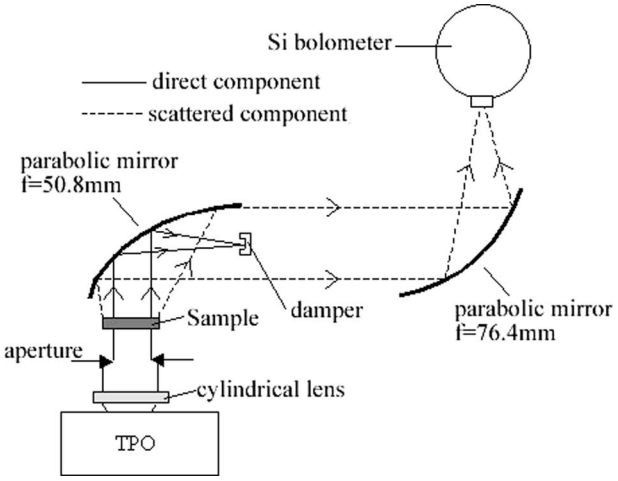

Fig. 17. *Schematic of the optical setup to measure the THz radiation scattered from powders.*

include THz chemical imaging) to verify whether or not it contains illegal substances.

To better understand the process of THz waves scattering from various powders, we built an imaging system similar to that described in [11], but modified to collect only scattered radiation. Sucrose powder separated by sieving into various grain sizes were placed in polyethylene bags and imaged at 617 GHz ($\lambda = 486$ μm). The result is shown in Fig. 18, and by plotting the average scattering intensity against the grain size we obtained the graph is Fig. 19. At grain sizes below 200 μm the scattering effect is very weak. Above this limit, the scattering can be detected for grain sizes above 1–2 mm; this range covers the grain size of usual illicit drugs.

With a similar optical setup, but using a frequency-multiplied microwave source that emits around 650 GHz (wavelength 461 μm), we imaged a sample consisting of sucrose powder (grain size 300–355 μm) arranged in the shape of letter R. Fig. 20(a) shows the image that we obtained; for the image in Fig. 20(b) the beam had to pass through a sheet of paper (an envelope) both ways, but still the image is very clear.

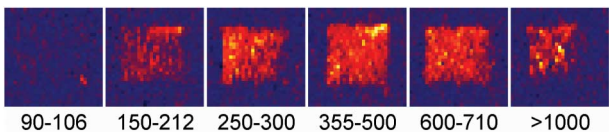

Fig. 18. *THz scattering images of sucrose bags with different grain sizes at 617 GHz. The grain size range is written below each image. (After [1].)*

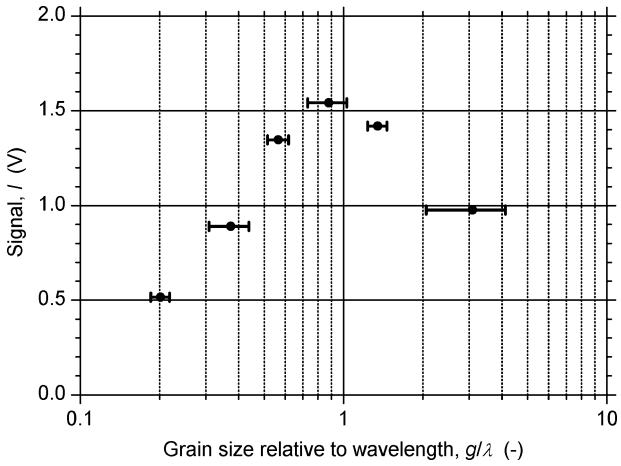

Fig. 19. *Plot showing the scattering efficiency as a function of the grain size given in units of wavelength* ($\lambda = 486$ μm). *The horizontal bars represent the grain size range for each sample. "Signal" is an average value calculated from the images in Fig. 18. (After [1].)*

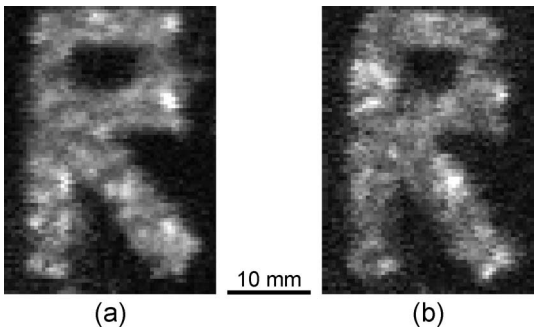

Fig. 20. *Sucrose powder arranged in the shape of letter* R, *imaged by collecting only the scattered radiation. The sample was imaged both (a) as is and (b) covered by a sheet of usual paper to simulate an envelope. (After [1].)*

VI. CONCLUSION

Although still at the beginning of a long road, the applications of THz waves have started to make visible progress, and the results shown here represent a part of our contribution to the field. A whole range of other homeland security applications are underway in several research groups around the world, and other directions such as medical diagnosis, agricultural monitoring, and industrial quality testing are already receiving much interest both from physics investigators and from the those specific communities.

Research on improving the THz-wave sources and detectors, performed in our group as well as elsewhere, will probably give the field more chances to find applications in everyday life. ■

REFERENCES

[1] A. Dobroiu, C. Otani, and K. Kawase, "Terahertz-wave sources and imaging applications," *Meas. Sci. Technol.*, vol. 17, pp. R161–R174, 2006.

[2] Y. Watanabe, K. Kawase, T. Ikari, H. Ito, Y. Ishikawa, and H. Minamide, *Appl. Phys. Lett.*, vol. 83, pp. 800–802, 2003.

[3] K. Kawase, Y. Ogawa, and Y. Watanabe, *Opt. Express*, vol. 11, pp. 2549–2554, 2003.

[4] X.-C. Zhang, *Phys. Med. Biol.*, vol. 47, pp. 3667–3677, 2002.

[5] S. S. Sussman, *Microwave Lab.*, Stanford Univ., Stanford, CA, Rep. 1851, 1970.

[6] M. A. Piestrup, R. N. Fleming, and R. H. Pantell, *Appl. Phys. Lett.*, vol. 26, p. 418, 1975.

[7] J. Shikata, K. Kawase, K. Karino, T. Taniuchi, and H. Ito, "Tunable terahertz-wave parametric oscillators using $LiNbO_3$ and MgO : $LiNbO_3$ crystals," *IEEE Trans. Microw. Theory Tech.*, vol. 48, no. 4, pt. 2, pp. 653–661, Apr. 2000.

[8] K. Kawase, J. Shikata, and H. Ito, *J. Phys. D, Appl. Phys.*, vol. 35, no. 3, p. R1, 2002.

[9] I. Shoji, T. Kondo, A. Kitamoto, M. Shirane, and R. Ito, *J. Opt. Soc. Amer. B*, vol. 14, p. 2268, 1997.

[10] K. Kawase, J. Shikata, H. Minamide, K. Imai, and H. Ito, *Appl. Opt.*, vol. 40, p. 1423, 2001.

[11] A. Dobroiu, M. Yamashita, Y. N. Ohshima, Y. Morita, C. Otani, and K. Kawase, *Appl. Opt.*, vol. 43, p. 5637, 2004.

[12] A. Dobroiu, R. Beigang, C. Otani, and K. Kawase, *Appl. Phys. Lett.*, vol. 86, p. 261 107, 2005.

[13] O. A. Simpson, B. L. Bean, and S. Perkowitz, *J. Opt. Soc. Amer.*, vol. 69, pp. 1723–1726, 1979.

[14] D. M. Wieliczka, S. Weng, and M. R. Querry, *Appl. Opt.*, vol. 28, pp. 1714–1719, 1989.

[15] M. R. Querry, D. M. Wieliczka, and D. J. Segelstein, *Handbook of Optical Constants of Solids II*. New York: Academic, 1991, pp. 1059–1077.

ABOUT THE AUTHORS

Adrian Dobroiu received the diploma in optical technology and the Ph.D. degree in physics from the University of Bucharest, Romania, in 1994 and 1999, respectively. His Ph.D. thesis was on self-calibrating algorithms in phase-shift interferometry.

Since 1994 he has successively held the positions of researcher at the Laser Department of the National Institute for Laser, Plasma and Radiation Physics, Romania, and postdoctoral fellow at the Yamagata University, Yonezawa, Japan, where he did research in the field of optical coherence tomography. Currently, he is a Researcher at the Institute for Physical and Chemical Research (RIKEN), Sendai, Japan, working on terahertz-wave imaging and other applications of terahertz radiation.

Dr. Dobroiu is a member of the Optical Society of America (OSA), the International Society of Optical engineering (SPIE), and the Japan Society of Applied Physics (JSAP).

Yoshiaki Sasaki received the B.Eng. degree in electrical engineering in 1995 from the Tohoku Institute of Technology, Sendai, Japan, and the Ph.D. degree from the Department of Bio-System Engineering of Yamagata University, Yonezawa, Japan, in 2004.

From 1996 to 1999, he was with the Biophoton Information Laboratories, Ltd., Yamagata, Japan, where he was a Research Scientist performing research on optical spectroscopy, optical imaging of biological tissue using the optical heterodyne detection method, and ultraweak light detection from living systems. From 1999 to 2001, he was a Laser Engineer with INDECO, Inc., Tokyo, Japan. Currently, he is with the Institute for Physical and Chemical Research (RIKEN), Sendai. His current research interests include detection of scattered THz waves from powders, THz imaging, and THz heterodyne detection.

Dr. Sasaki is a member of the Optical society of America (OSA) and the Japan Society of Applied Physics (JSAP).

Takayuki Shibuya received the B.S. degree from the Tokyo University of Science, Tokyo, Japan, in 2004. He is currently working toward the M.S. degree at the same university.

He is also a Student Trainee at the Institute of Physical and Chemical Research (RIKEN), Sendai, Japan, where he is involved in the research on the development of terahertz-wave sources based on nonlinear optical crystals.

Chiko Otani received the B.S. degree in physics from Kyoto University, Kyoto, Japan, in 1990 and the M.S. and Ph.D. degrees in astronomy from the University of Tokyo, Tokyo, Japan, in 1992 and 1995, respectively.

Since 1995, he has successively worked in the Cosmic Radiation Laboratory and the Image Information Division of the Institute of Physical and Chemical Research (RIKEN), Wako, Japan, and is currently a Postdoctoral Researcher with the Kawase Initiative Research Unit, RIKEN. His research interests include the development of superconducting radiation detectors and their applications in the terahertz region.

Dr. Otani is a member of the Astronomical Society of Japan, the Physical Society of Japan, and the Japan Society of Applied Physics (JSAP).

Kodo Kawase (Member, IEEE) was born in Kyoto, Japan, on September 14, 1966. He received the B.S. degree in electronic engineering from Kyoto University, Kyoto, in 1989 and the M.S. and Ph.D. degrees in electronic engineering from Tohoku University, Sendai, Japan, in 1992 and 1996, respectively.

From 1989 to 1990, he was with the Research Development Corporation of Japan (JRDC). In 1996, he became a COE Researcher at the Research Institute of Electrical Communication, Tohoku University. In 1997 and 1998, he became a Research Associate and an Assistant Professor at Tohoku-Gakuin University, respectively. In 1999, he became a Sub-Team Leader at Photo Dynamics Research Center, Institute of Physical and Chemical Research (RIKEN), Sendai. In 2001, he became a Research Unit Leader at RIKEN, Wako, Japan. In 2004, he became a Visiting Professor of Graduate School of Agricultural Science, Tohoku University. Since July 2005, he has been a Professor of the Graduate School of Engineering, Nagoya University, Nagoya, Japan. Since 1992, he has been involved in research on terahertz-wave generation using nonlinear optics.

Dr. Kawase is a member of the Japan Society of Applied Physics (JSAP), the Laser Society of Japan, the Institute of Electronics, Information and Communication Engineers (IEICE), Japan, and the Optical Society of America (OSA). He received the 1997 Young Scientist Award for the Presentation of an Excellent Paper presented by the JSAP, Japan, the 1998 Award for the Excellent Presentation presented by the Laser Society of Japan, the 2000 Prize of Laser Engineering, the Medal of Excellent Paper presented by the Laser Society of Japan, the 2002 Marubun Research and Encouragement Award by the Marubun Research Promotion Foundation (MRPF), and the 2005 Young Scientists' Prize by the Commendation for Science and Technology by the Minister of Education, Culture, Sports, Science and Technology (MEXT).